SUPPORTING INFORMATION

Protonation-Induced Room Temperature Phosphorescence in Fluorescent Polyurethane

Wei Sun,[a] Zhaowu Wang,[b,c] Tao Wang,[a] Li Yang,[b,c] Jun Jiang,*[b,c] Xingyuan Zhang,*[a] Yi Luo[b,c] and Guoqing Zhang*[b]

[a.] CAS Key Laboratory of Soft Matter Chemistry, Department of Polymer Science and Engineering, University of Science and Technology of China, Hefei, 230026 Anhui, P.R.China.

[b.] Hefei National Laboratory for Physical Sciences at the Microscale, University of Science and Technology of China, 96 Jinzhai Road, Hefei, Anhui, 230026, P.R.China.

[c.] Innovation Center of Chemistry for Energy Materials, Department of Chemical Physics, University of Science and Technology of China, Hefei, 230026 Anhui, P.R.China.

E-mail: gzhang@ ustc.edu.cn

Part I. Synthesis of F1 and Covalent Dye-Polymer Conjugate F1-PUs

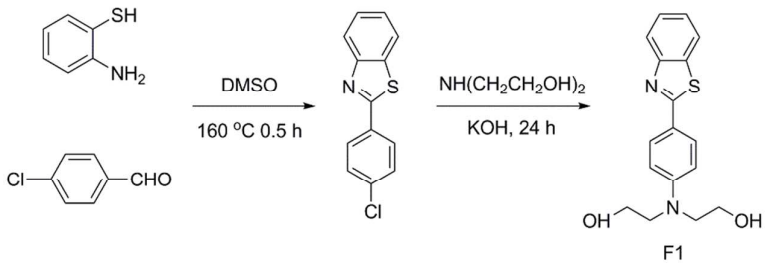

Chart S1. Synthesis of fluorescent dye **F1**.

Table S1. Chemical composition for the reaction to obtain **F1-PU**.

Sample	**F1-PU**
PTMG/g	6.5
IPDI/g	4.3
MDEA/g	1.2
BDO/g	0.19
Thioflavine (**F1**)/g	0.65
MDEA (%)	9.35%
F1 (%)	5%

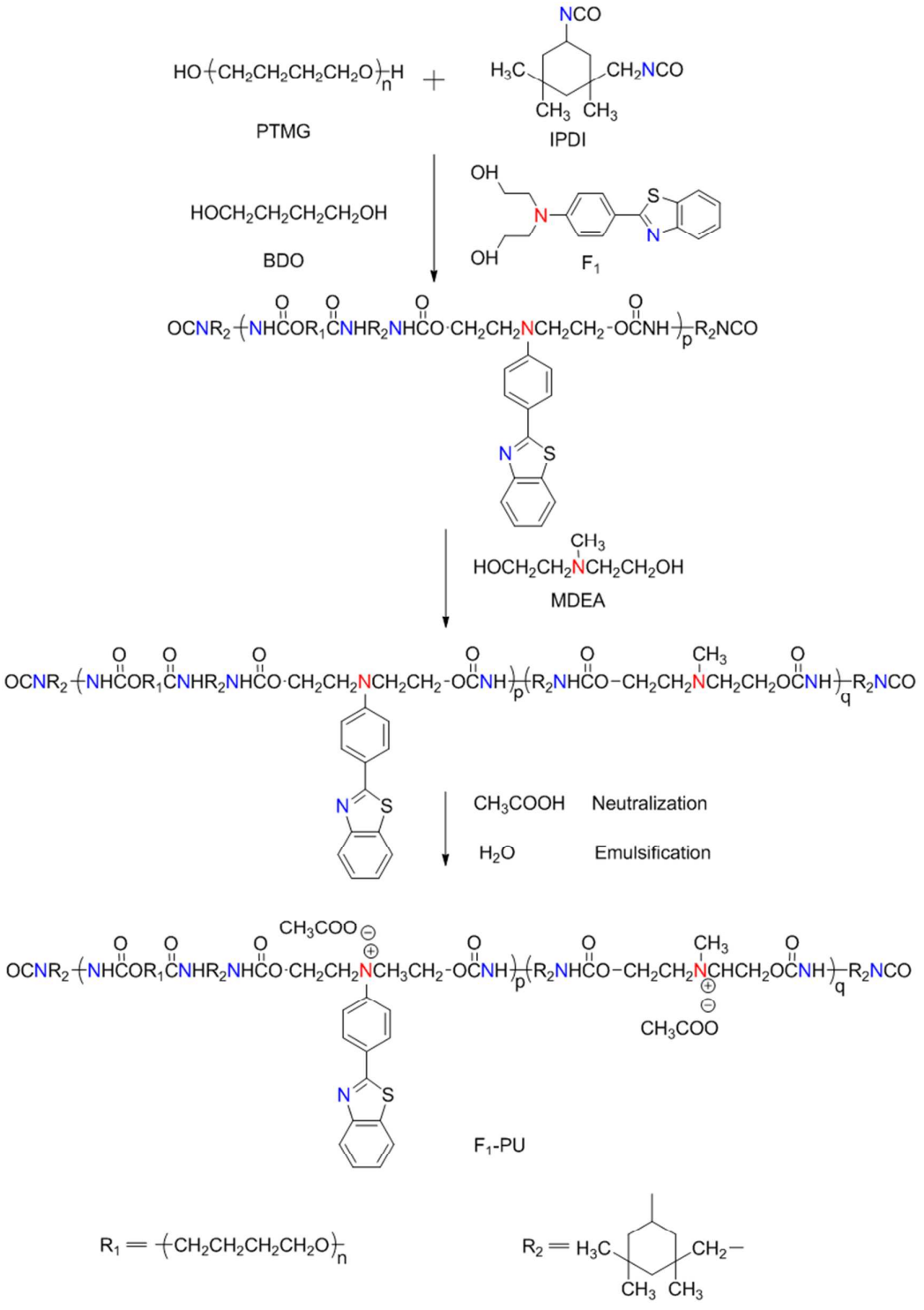

Chart S2. Synthesis of dye-polymer conjugate **F1-PU**

Part II. NMR and MS Figures

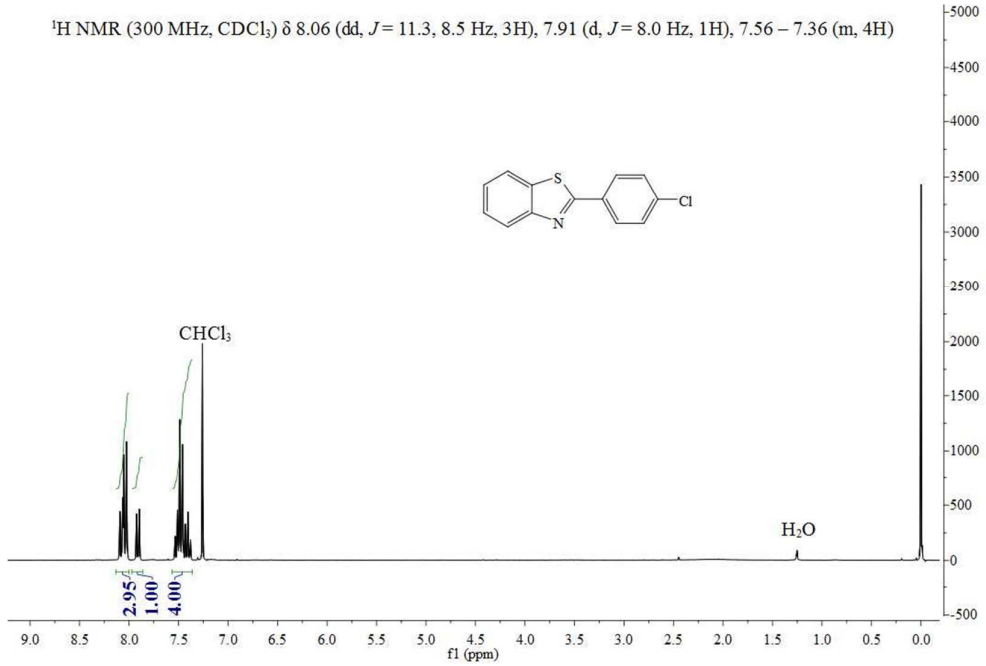

Figure S1. ^{1}H-NMR spectrum of D1 (300 MHz, $CDCl_3$, 298 K)

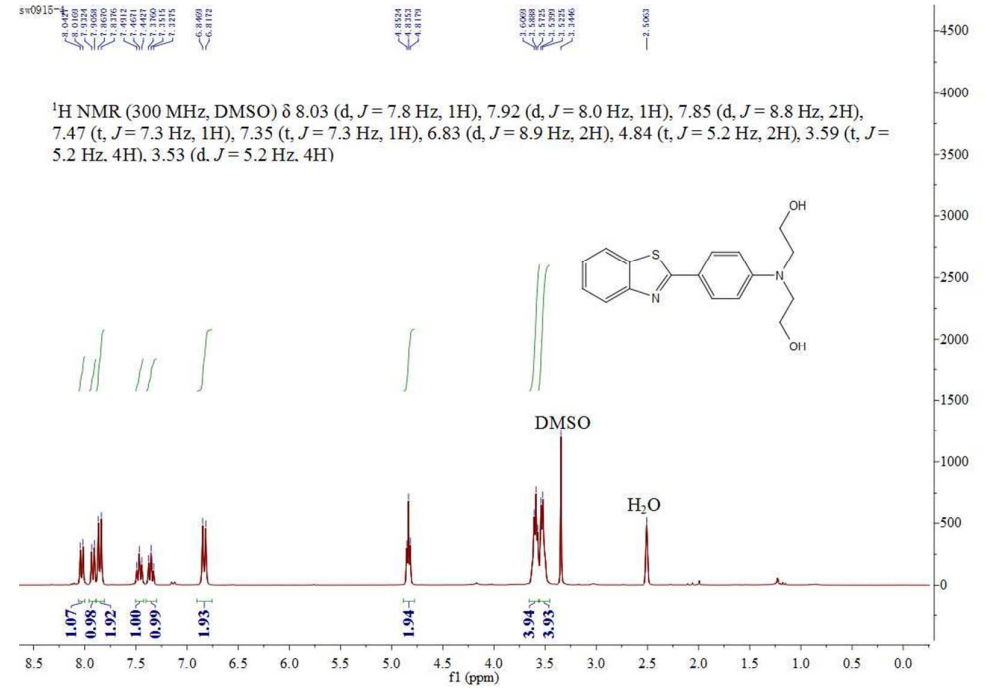

Figure S2. ^{1}H-NMR spectrum of F1 (300 MHz, DMSO, 298 K)

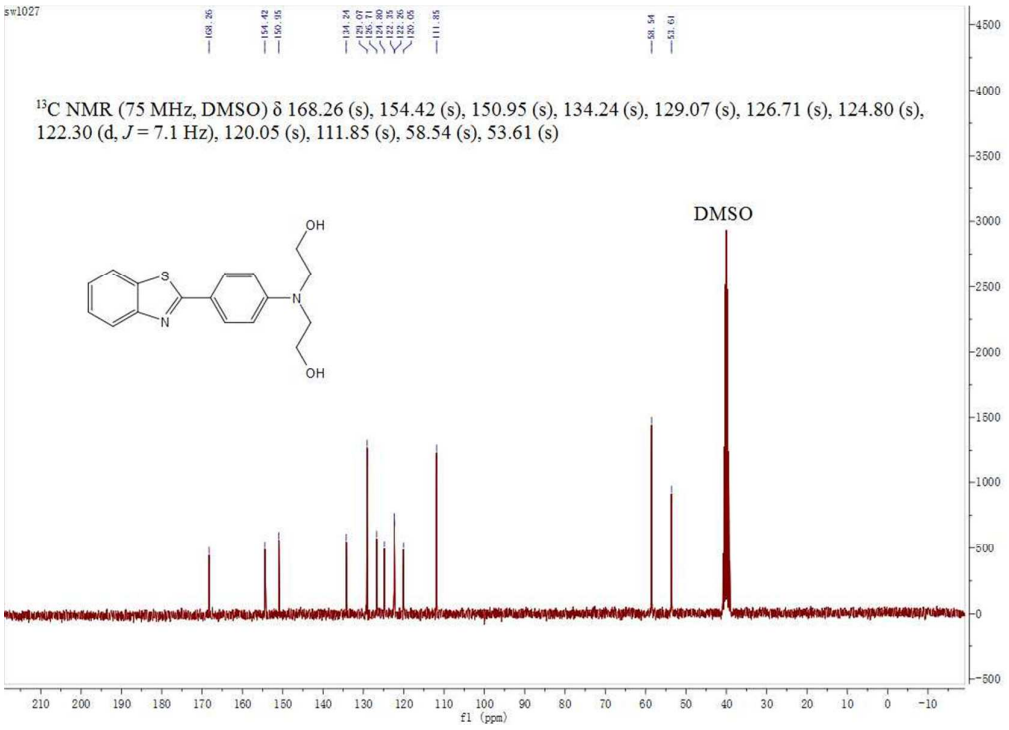

Figure S3. ^{13}C-NMR spectrum of F1 (300 MHz, DMSO, 298 K).

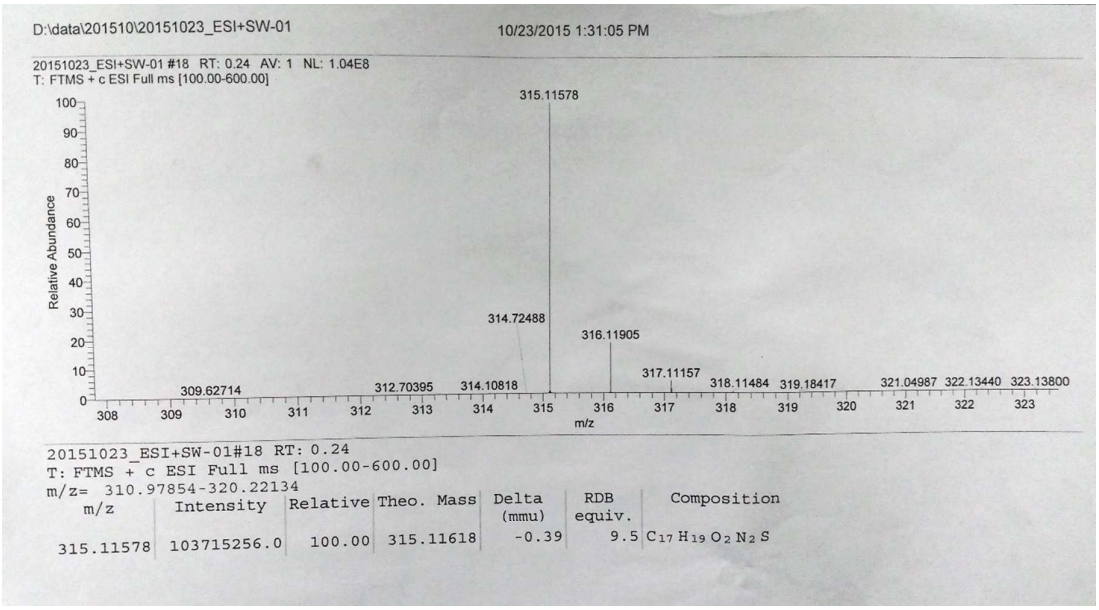

Figure S4. HRMS (MALDI-TOF) spectrum of F1 (300 MHz, DMSO, 298 K).

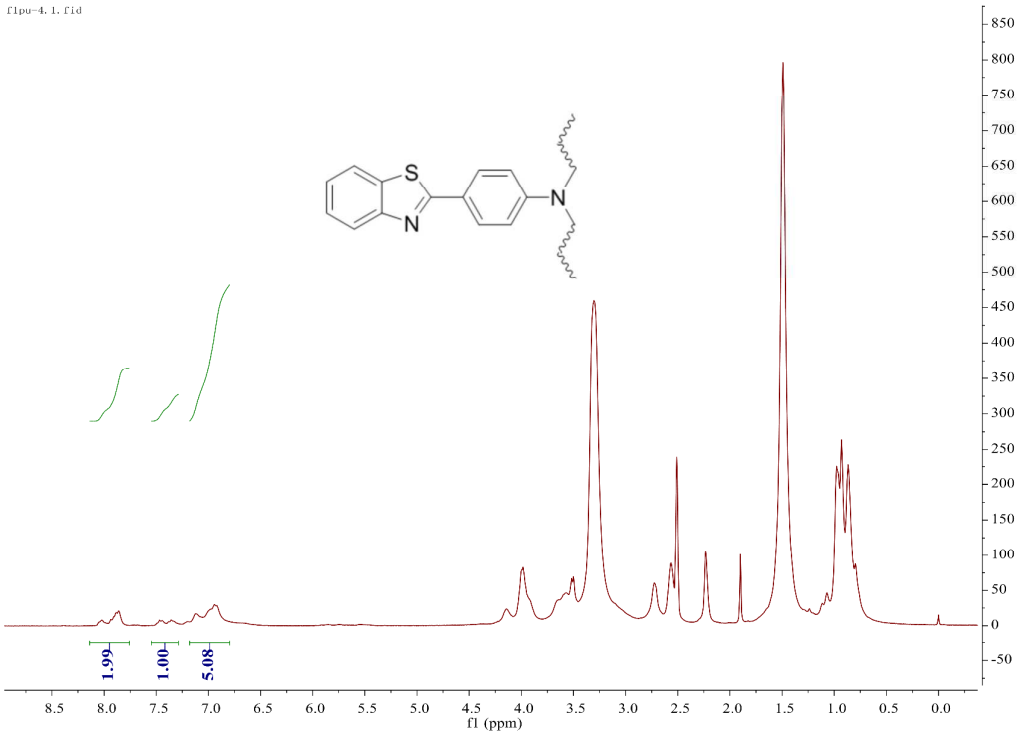

Figure S5. ^{1}H-NMR spectrum of F1-PU (300 MHz, DMSO, 298 K).

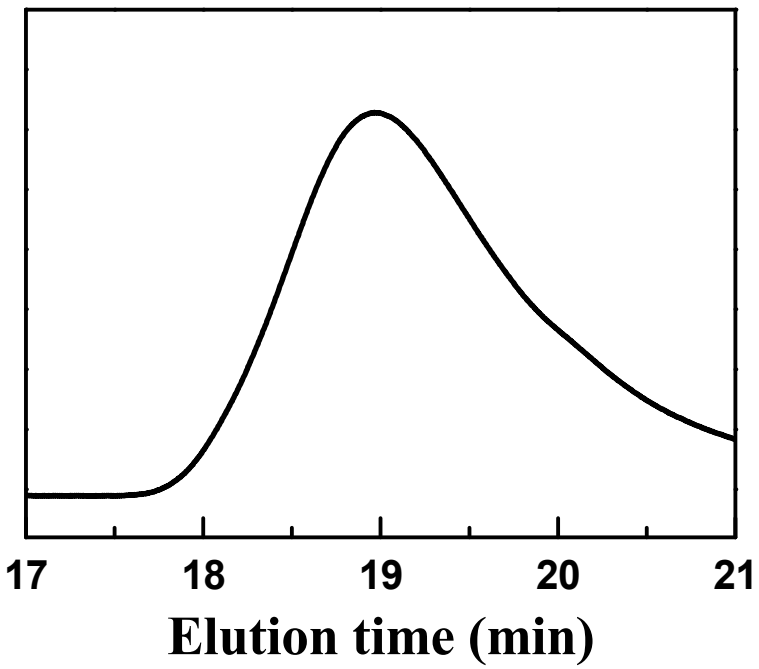

Figure S6. GPC graphic of F1-PU

Part III. Supporting Tables and Figures.

Table S2. Fluorescence characterization of **F1-PU** with different molar ratio of benzenesulfonic acid and F1 in DCM.

Molar ratio[a]	No acid	0.6:1	1.7:1	3.9:1	6.1:1	8.3:1	10.4:1	12.6:1
Lifetime[b]	1.57 ns	1.51 ns	1.91 ns	1.96 ns	1.99 ns	2.00 ns	1.92 ns	1.83 ns
λ_{em}[c]	411 nm	411 nm	461 nm	462 nm	462 nm	462 nm	462 nm	462 nm
λ_{ex}[d]	355 nm	355 nm	429 nm	429 nm	429 nm	429 nm	429 nm	429 nm

[a]Molar ratio between BA and **F1**. [b]Weight-averaged fluorescence lifetime. [c]Emission maxima excited at 365nm. [d]Excitation maxima excited at emission maxima.

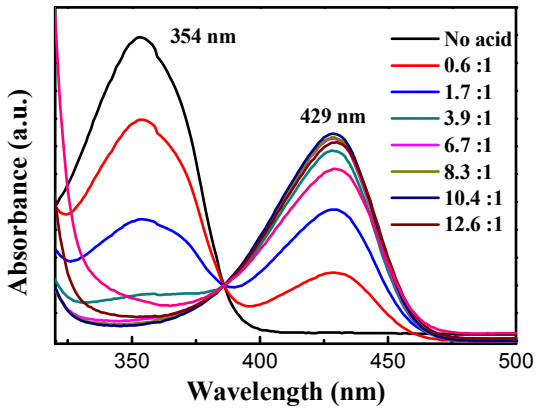

Figure S7. UV-Vis absorption spectra of **F1-PU** in the presence of various ratios of benzenesulfonic acid in dichloromethane.

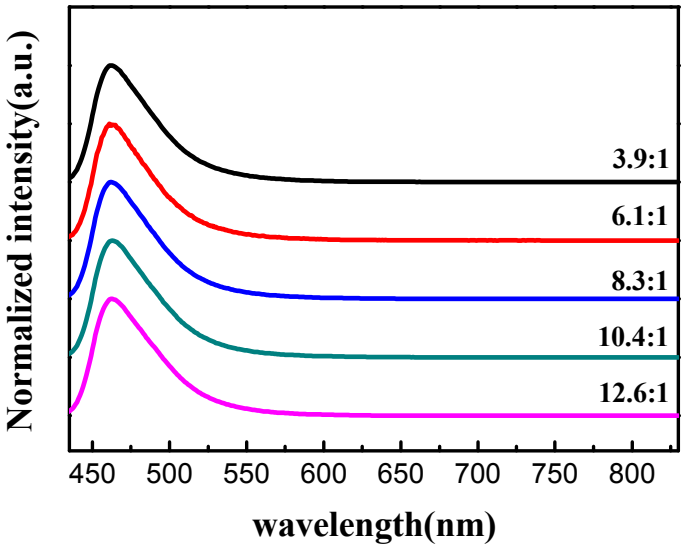

Figure S8. Normalized steady-state emission spectra of F1-PU with the presence of various molar ratios of benzenesulfonic acid in dichloromethane ([F1] = 10^{-4} M; λ_{ex} = 429 nm).

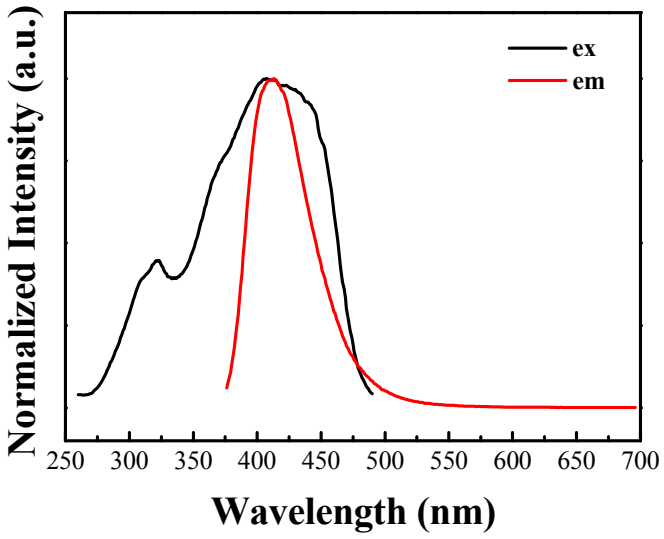

Figure S9. Normalized steady-state excitation spectrum of $F1H^+$ and emission spectrum of F1.

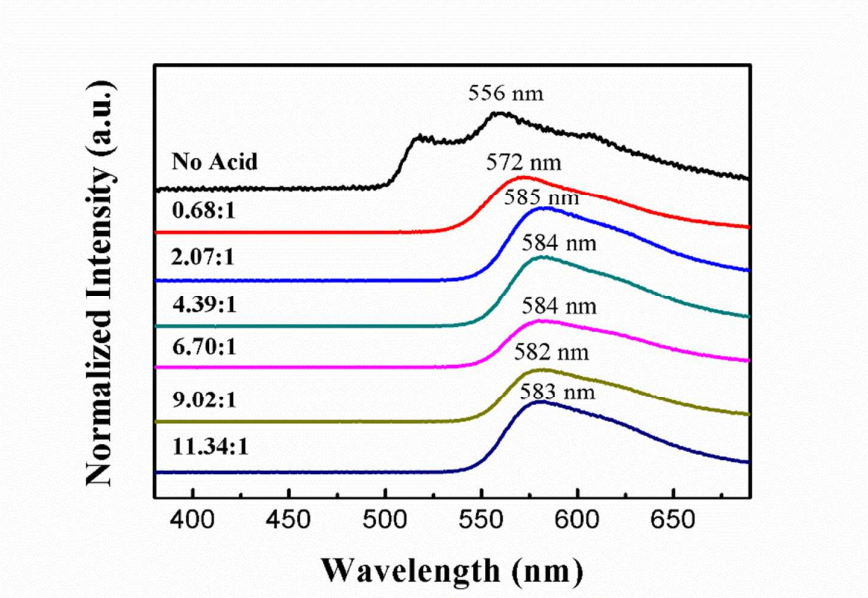

Figure S10. Delayed emission spectra at 77 K for **F1-PU** films at different BA ratios (Δt = 10 ms).

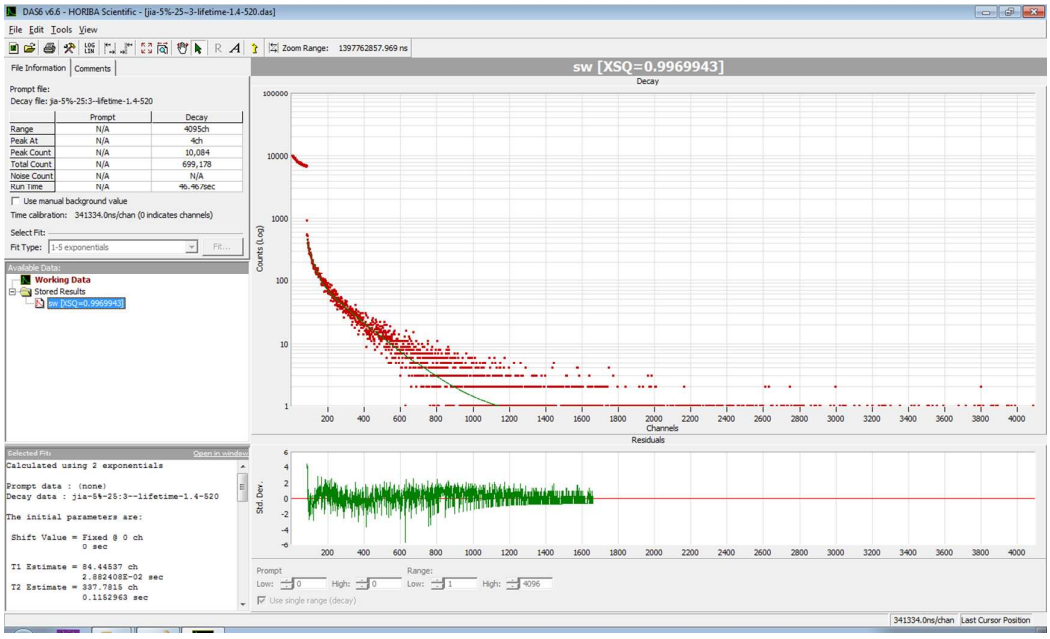

Figure S11. Graphic data of the lifetime test of **F1-PU** with BA (0.68 eq.)

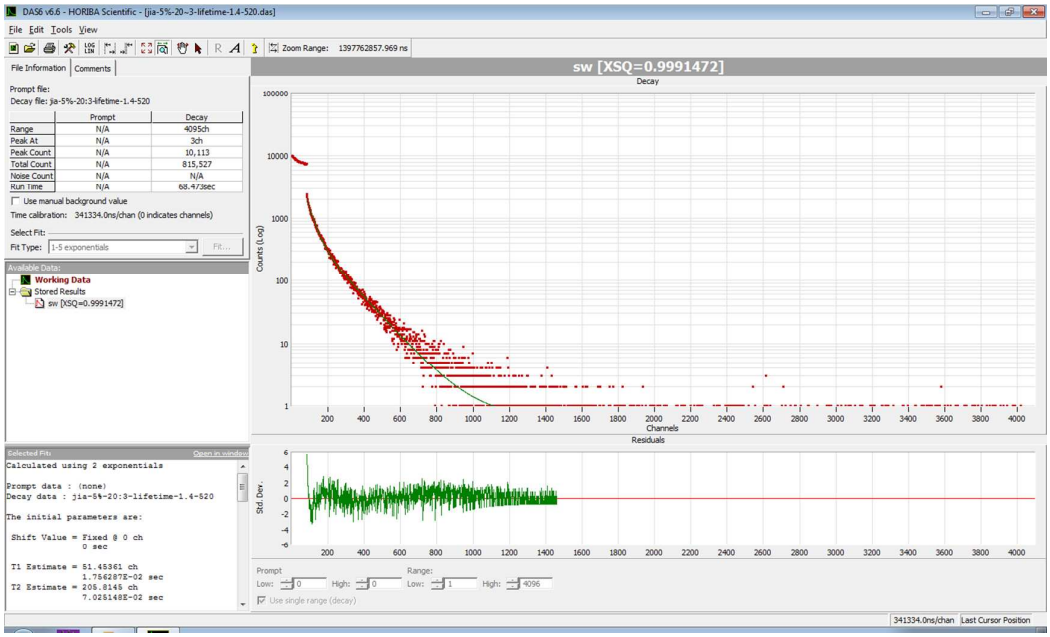

Figure S12. Graphic data of the lifetime test of **F1-PU** with BA (2.07 eq.)

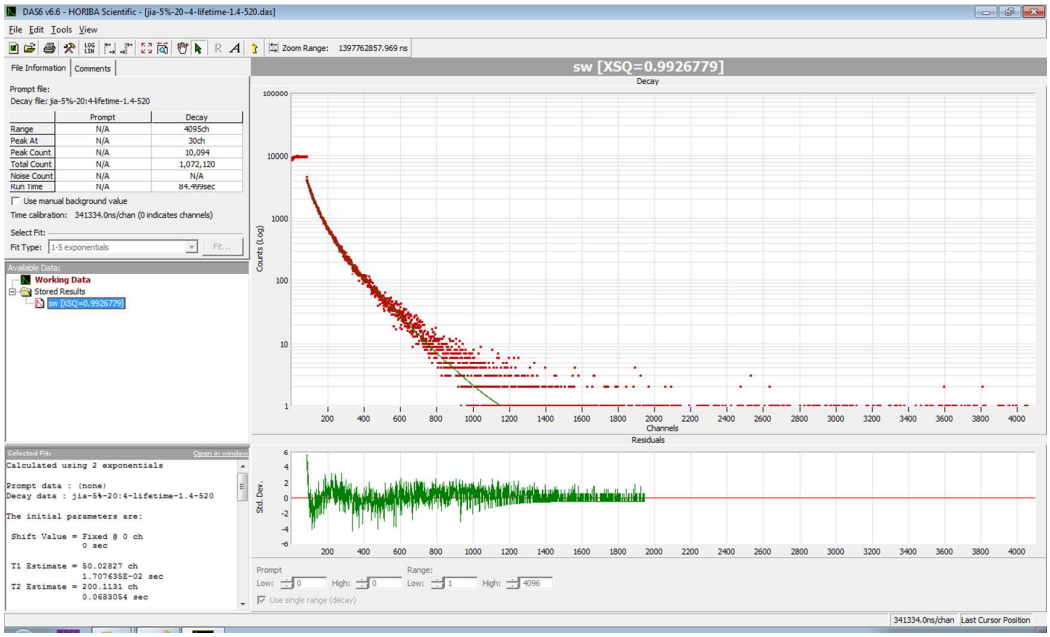

Figure S13. Graphic data of the lifetime test of **F1-PU** with BA (4.39 eq.)

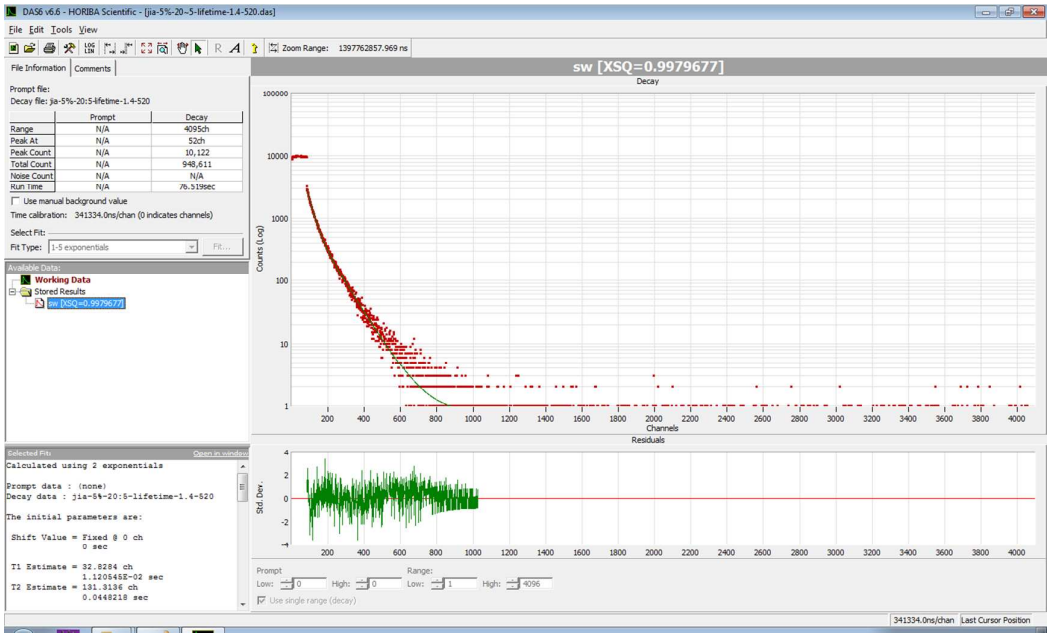

Figure S14. Graphic data of the lifetime test of **F1-PU** with BA (6.70 eq.)

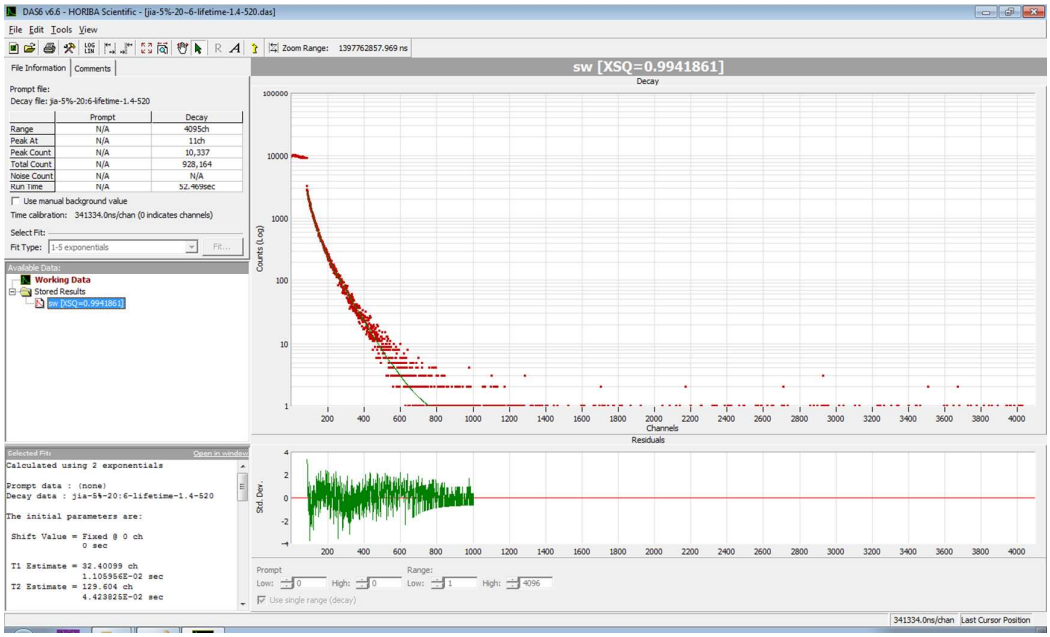

Figure S15. Graphic data of the lifetime test of **F1-PU** with BA (9.02 eq.)

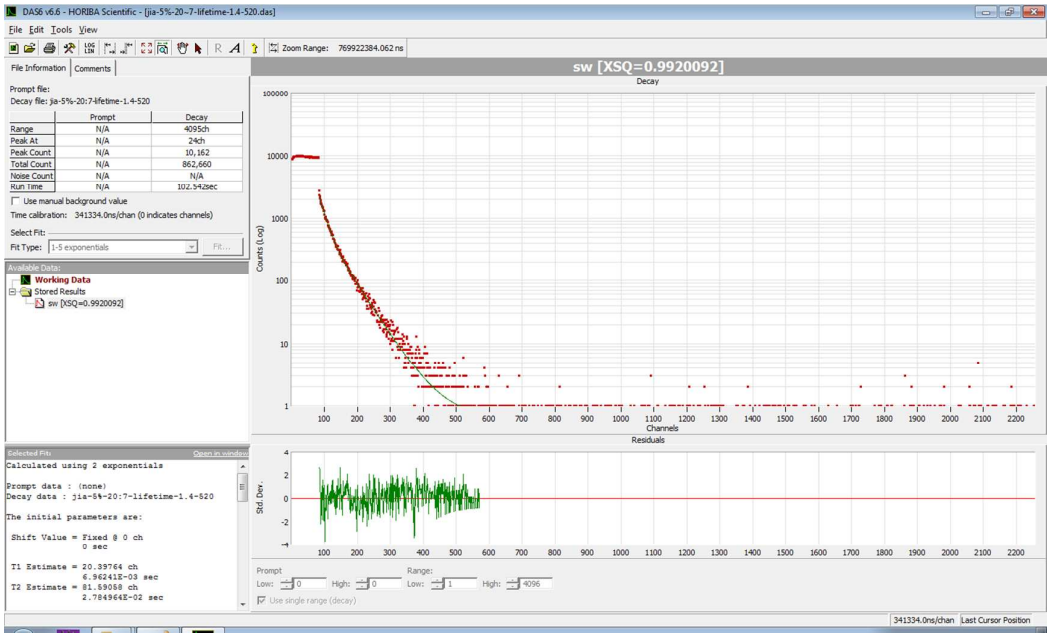

Figure S16. Graphic data of the lifetime test of **F1-PU** with BA (11.34 eq.)

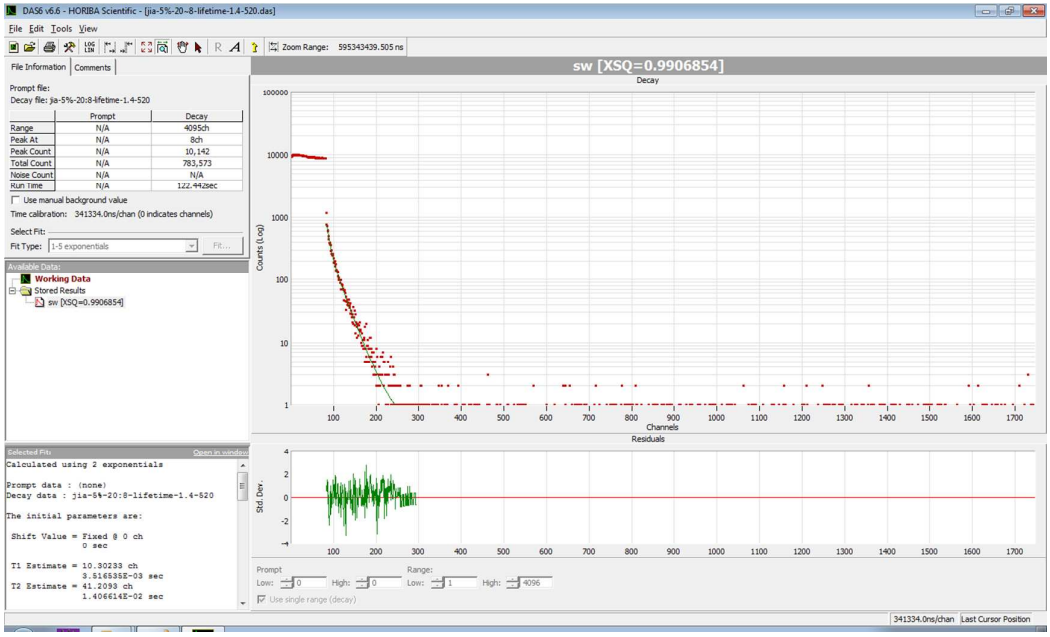

Figure S17. Graphic data of the lifetime test of **F1-PU** with BA (13.66 eq.)

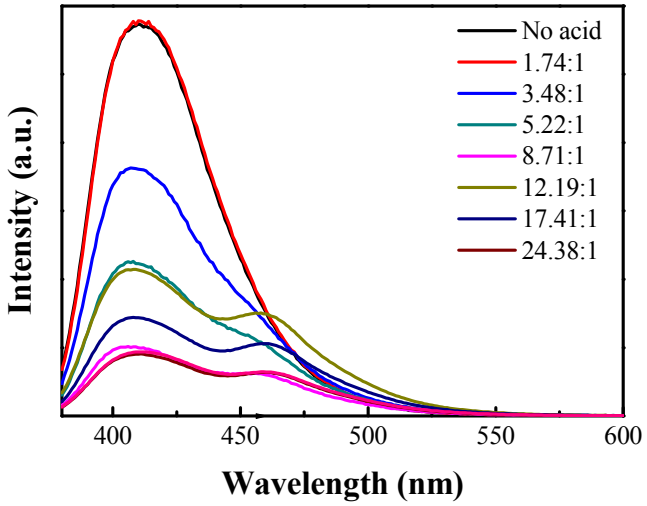

Figure S18. Steady-state fluorescence emission spectra of F1 in the presence of various ratios of benzenesulfonic acid in dichloromethane.

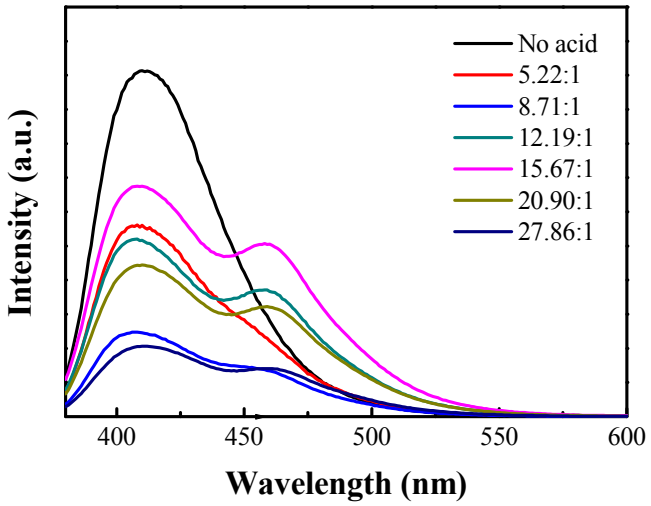

Figure S19. Steady-state fluorescence emission spectra of F1-doped PU and various ratios of benzenesulfonic acid in dichloromethane.

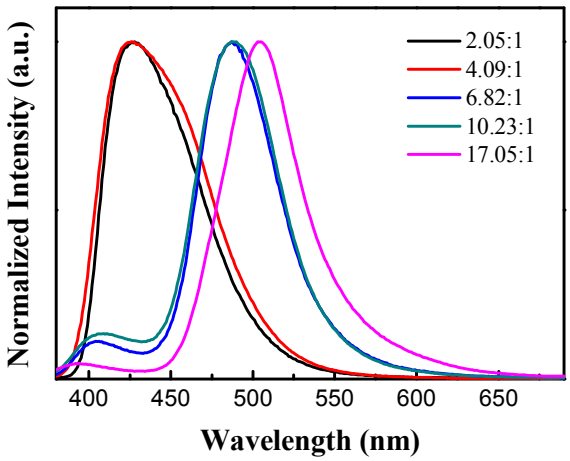

Figure S20. Normalized steady-state fluorescence emission spectra of F1 doped PU and various ratios of benzenesulfonic acid in the solid state.

For the spectra obtained in solution, they are given as un-normalized formation. As for the spectra obtained for solid films, normalized spectra are given due to the random intensity fluctuation for solid-state measurement (this is a well-known problem, where a slight rotation of the solid-state sample can result in intensity change).

Polyurethane is a very polar polymer which is able to host protic acids without causing significant phase separation. In other words, the polymer chain can enhance the local proton concentration near the fluorophore. For example, in CH_2Cl_2, F1 alone (Fig. R18) or its non-covalent blending with PU (Fig. R19) does not exhibit dramatic emission change while F1-PU (Fig. 1b in manuscript) exhibits much more pronounced change.

As for the F1-doped PU in the solid state, the PL emission spectra behave quite differently vs. the covalently attached F1-PU in the presence of various ratios of acids. We attribute the difference to dye aggregation effects which more dramatically shift the emission spectra (Figure R20). This could be evidenced by visual aggregation particles observed. Using isolated dye/PU mixture can complicate the results and conclusion and it has been excluded from the current study.

Table S3. Luminescence characterization of F1-PU thin films with different molar ratios of benzenesulfonic acid (BA) and F1 in air and in vacuum at room temperature.

Ratio	Lifetime (air)		Lifetime (vacuum)	
No acid	1.52 ns	1.366231×10^{-9} s (88.73%) 2.751761×10^{-9} s (11.27%)	1.59 ns	1.067345×10^{-9} s (78.07%) 2.085114×10^{-9} s (21.93%)
0.68:1	2.32 ns	1.173635×10^{-9} s (65.58%) 3.04766×10^{-9} s (28.31%) 1.127998×10^{-8} s (6.11%)	45.6 ms	9.700042×10^{-3} s (31.04%) 6.178555×10^{-2} s (68.96%)
2.07:1	1.65 ns	1.650215×10^{-9} s (40.35%) 3.367669×10^{-10} s (44.57%) 5.5562×10^{-9} s (15.07%)	32.7 ms	1.288959×10^{-2} s (42.00%) 4.709332×10^{-2} s (58.00%)
4.39:1	1.43 ns	1.4276×10^{-9} s (35.25%) 2.710821×10^{-10} s (47.86%) 4.704123×10^{-9} s (16.89%)	32.8 ms	1.566402×10^{-2} s (48.72%) 4.911054×10^{-2} s (51.28%)
6.70:1	1.79 ns	5.732946×10^{-10} s (49.03%) 1.944192×10^{-9} s (35.73%) 5.331289×10^{-9} s (15.25%)	23.1 ms	1.061586×10^{-2} s (41.89%) 3.215964×10^{-2} s (58.11%)
9.02:1	1.62 ns	5.651365×10^{-10} s (55.02%) 2.000652×10^{-9} s (31.93%) 5.155282×10^{-9} s (13.05%)	21.2 ms	9.982257×10^{-3} s (45.34%) 3.055979×10^{-2} s (54.66%)
11.34:1	1.38 ns	5.507013×10^{-10} s (62.90%) 1.874215×10^{-9} s (26.66%) 4.772416×10^{-9} s (10.45%)	13.4 ms	6.402263×10^{-3} s (42.36%) 1.862563×10^{-2} s (57.64%)
13.66:1	1.34 ns	5.404025×10^{-10} s (62.42%) 1.750683×10^{-9} s (27.01%) 4.632095×10^{-9} s (10.56%)	6.66 ms	5.704241×10^{-3} s (36.57%) 1.623003×10^{-2} s (63.43%)

Part IV. Calculated information

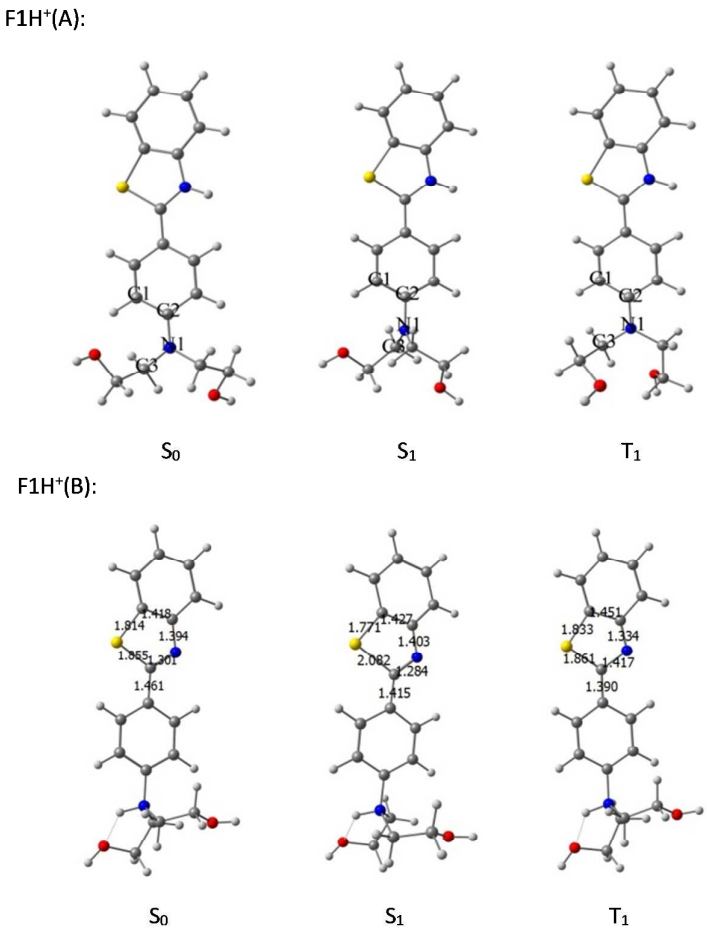

Figure S21. The molecular structures of S_0, S_1 and T_1 for **F1H$^+$(A)** and **F1H$^+$(B)**.

The clear excitation-induced structural variations were observed at the tail group of N-(CH_2-CH_2-OH)$_2$ by the structures of S_0, S_1 and T_1 of **F1H$^+$(A)** and **F1H$^+$(B)**. For

$F1H^+$(A), the dihedral angle as marked by atom C1, C2, N1 and C3 is close to zero at the ground state S_0, which was turned to be 88° in S_1 and moved back to -2.4° in T_1. While for **$F1H^+$(B)**, the structure is not very sensitive to the excitations.

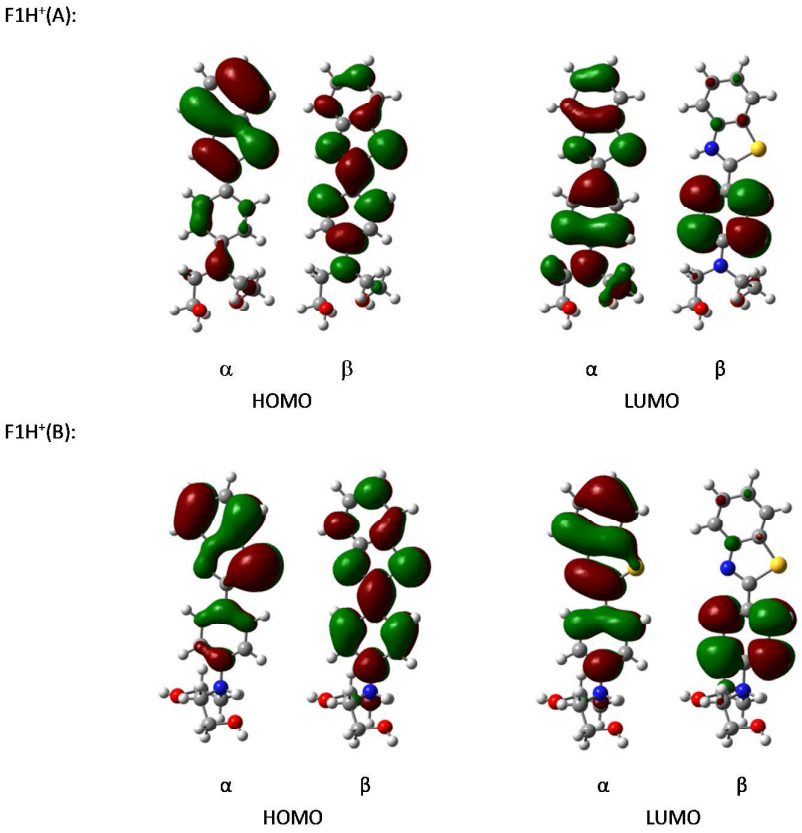

Figure S22. The HOMO and LUMO wavefunction of the lowest triplet state T_1 for $F1H^+$(A) and $F1H^+$(B). Here α and β stand for spin up and down orbitals, respectively.

The wavefunction distribution of HOMO and LUMO of the T_1 state in **$F1H^+$(A)** and **$F1H^+$(B)** can suggest a charge transfer character.

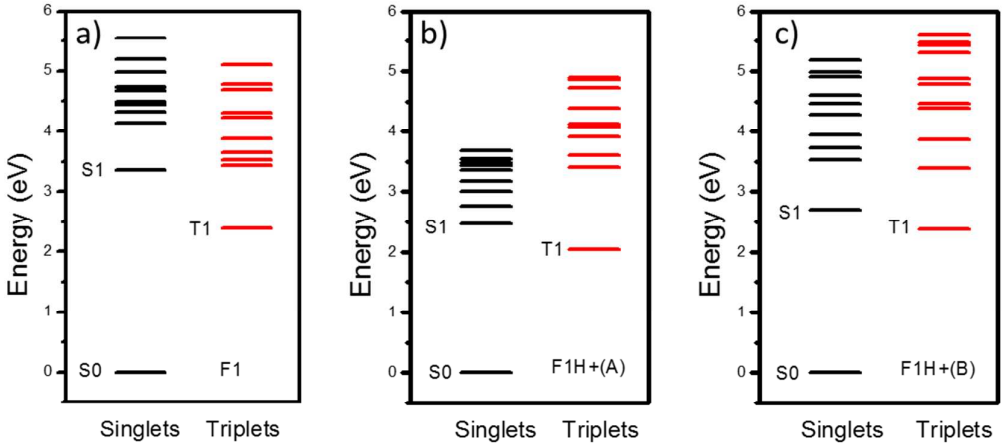

Figure S23. The computed singlet and triplet excited electronic energy levels of F1, $F1H^+$(A) and $F1H^+$(B).

The high-order triplet states of thioflavin with and without protonation are computed and presented (Figure S10), which could facilitate the intersystem crossing process. It is found that the high-order triplet state (above the lowest one of T_1) of thioflavin with and without protonation hold energy higher than the lowest singlet excited state S_1, suggesting that the intersystem crossing rates from S_1 to the high-order triplet states are relatively low and we can thus ignore their influence in this study.

Table S4. Natural Bond Orbital (NBO) analysis of the electronic transition for the lowest excited state S1 in F1.

NBO analysis of HOMO:

Orbital Number	Orbital combination	coefficient	Ratio
3（BD）	C1-C6	0.2012	0.0405
6（BD）	C2-C3	0.1298	0.0168
11（BD）	C4-C5	0.2047	0.0419
18（BD）	C7-N36	-0.2565	0.0658
22（BD）	C8-C10	0.3904	0.1524
24（BD）	C9-C11	-0.1583	0.0250
31（BD）	C12-C13	0.3826	0.1464
34（BD）	C14-C15	0.1037	0.0110
41（BD）	C16-C17	0.1061	0.0113
Total			0.5111

NBO analysis of LUMO:

Orbital Number	Orbital combination	coefficient	Ratio
192（BD*）	C1-C6	0.3114	0.0970
207（BD*）	C2-C3	0.5771	0.3330
211（BD*）	C4-C5	0.3345	0.1119
213（BD*）	C7-N36	0.1916	0.0367
220（BD*）	C8-C10	0.2544	0.0647
Total			0.6433

It is found that about 51.1% of HOMO is attributed to π bond and 64.3% of LUMO is attributed to π bond, demonstrating the dominant electronic transition as the π-π* feature.

Table S5. Natural Bond Orbital (NBO) analysis of the electronic transition for the lowest excited state S1 in $F1H^{+}$(A).

NBO analysis of HOMO:

Orbital Number	Orbital combination	coefficient	Ratio
82（LP）	O39	0.8678	0.7531

NBO analysis of LUMO:

Orbital Number	Orbital combination	coefficient	Ratio
76（LP^{*}）	C7	0.5682	0.3229
77（LP^{*}）	N36	0.3436	0.1181
80（LP^{*}）	S38	0.3362	0.1130
Total			0.554

It is found that about 75.3% of HOMO is attributed to n bond and 55.4% of LUMO is attributed to n* bond, demonstrating the dominant electronic transition as the n-n* feature.

Table S6. Natural Bond Orbital (NBO) analysis of the electronic transition for the lowest excited state S1 in $F1H^{+}$(B).

NBO analysis of HOMO:

Orbital Number	Orbital combination	coefficient	Ratio
8（BD）	C3-C4	0.5788	0.3350
13（BD）	C5-C6	0.4694	0.2203
18（BD）	C7-N36	0.35	0.1225
Total			0.6778

NBO analysis of LUMO:

Orbital Number	Orbital combination	coefficient	Ratio
208（BD^{*}）	C7-N36	0.4732	0.2239
211（BD^{*}）	C8-C9	0.465	0.2162
219（BD^{*}）	C11-C13	0.4357	0.1899
Total			0.63

It is found that about 67.8% of HOMO is attributed to π bond and 63% of LUMO is attributed to π* bond, demonstrating the dominant electronic transition as the π-π* feature.